Journal of Hydrology 603 (2021) 126854

Contents lists available at ScienceDirect

Journal of Hydrology

journal homepage: www.elsevier.com/locate/jhydrol

A hybridized model based on neural network and swarm intelligence-grey wolf algorithm for spatial prediction of urban flood-inundation

Hamid Darabi [a,*], Ali Torabi Haghighi [a], Omid Rahmati [b], Abolfazl Jalali Shahrood [a], Sajad Rouzbeh [c], Biswajeet Pradhan [d,f,g,*], Dieu Tien Bui [e,*]

[a] Water, Energy and Environmental Engineering Research Unit, University of Oulu, P.O. Box 4300, FIN-90014, Oulu, Finland
[b] Soil Conservation and Watershed Management Research Department, Kurdistan Agricultural and Natural Resources Research and Education Center, AREEO, Sanandaj, Iran
[c] Department of Watershed Management, Sari Agriculture Science and Natural Resources University, P.O. Box 737, Sari, Iran
[d] Center for Advanced Modeling and Geospatial Information Systems (CAMGIS), Faculty of Engineering and Information Technology, University of Technology Sydney, NSW 2007, Australia
[e] GIS Group, Department of Business and IT, University of South-Eastern Norway, Gullbringvegen 36, N-3800 Bø i Telemark, Norway
[f] Department of Energy and Mineral Resources Engineering, Sejong University, Choongmu-gwan, 209 Neungdong-ro, Gwangjin-gu, Seoul 05006, Korea
[g] Earth Observation Center, Institute of Climate Change, Universiti Kebangsaan Malaysia, 43600 UKM, Bangi Selangor, Malaysia

ARTICLE INFO

This manuscript was handled by Nandita Basu, Editor-in-Chief, with the assistance of Andrea E. Brookfield, Associate Editor

Keywords:
Flood inundation
Flood inventory
GIS
NN-SGW model
Confusion matrix

ABSTRACT

In regions with lack of hydrological and hydraulic data, a spatial flood modeling and mapping is an opportunity for the urban authorities to predict the spatial distribution and the intensity of the flooding. It helps decision-makers to develop effective flood prevention and management plans. In this study, flood inventory data were prepared based on the historical and field surveys data by Sari municipality and regional water company of Mazandaran, Iran. The collected flood data accompanied with different variables (digital elevation model and slope have been considered as topographic variables, land use/land cover, precipitation, curve number, distance to river, distance to channel and depth to groundwater as environmental variables) were applied to novel hybridized model based on neural network and swarm intelligence-grey wolf algorithm (NN-SGW) to map flood-inundation. Several confusion matrix criteria were used for accuracy evaluation by cutoff-dependent and independent metrics (e.g., efficiency (E), positive predictive value (PPV), negative predictive value (NPV), area under the receiver operating characteristic curve (AUC)). The accuracy of the flood inundation map produced by the NN-SGW model was compared with that of maps produced by four state-of-the-art benchmark models: random forest (RF), logistic model tree (LMT), classification and regression trees (CART), and J48 decision tree (J48DT). The NN-SGW model outperformed all benchmark models in both training (E = 90.5%, PPV = 93.7%, NPV = 87.3%, AUC = 96.3%) and validation (E = 79.4%, PPV = 85.3%, NPV = 73.5%, AUC = 88.2%). As the NN-SGW model produced the most accurate flood-inundation map, it can be employed for robust flood contingency planning. Based on the obtained results from NN-SGW model, distance from channel, distance from river, and depth to groundwater were identified as the most important variables for spatial prediction of urban flood inundation. This work can serve as a basis for future studies seeking to predict flood susceptibility in urban areas using hybridized machine learning (ML) models and can also be applied in other urban areas where flood inundation presents a pressing challenge, and there are some problems regarding required model and availability of input data.

1. Introduction

Floods occur due to a sudden rise in river water levels caused by snowmelt or intense precipitation (Peyravi et al., 2019), or to failure of a hydraulic structure (e.g., Ashley and Ashley, 2008). Catastrophic local flooding has been reported throughout the world, e.g. the Giofyros River

* Corresponding authors at: Center for Advanced Modeling and Geospatial Information Systems (CAMGIS), Faculty of Engineering and Information Technology, University of Technology Sydney, NSW 2007, Australia (B. Pradhan).
E-mail addresses: Hamid.darabi@oulu.fi (H. Darabi), Biswajeet.Pradhan@uts.edu.au (B. Pradhan), dieu.t.bui@usn.no (D. Tien Bui).

https://doi.org/10.1016/j.jhydrol.2021.126854
Received 24 February 2021; Received in revised form 4 June 2021; Accepted 17 August 2021
Available online 24 August 2021

in Greece in 1994, the Aude River in France in 1999, and the Trisanna River in Austria in 2005 (Marchi et al., 2010). Previous studies have considered flooding as a natural hazard in fluvial systems and have examined flash floods along floodplains (Hosseini et al., 2020), but less attention has been paid to urban flooding (Chen et al., 2009). Urban areas are prone to flooding owing to their widespread use of impervious materials for rooftops, streets, and roads (Schubert and Sanders, 2012; Pirnia et al., 2019), which is known to increase the volume and rate of surface runoff (Shuster et al., 2005; Du et al., 2015). Climate change and its impact on the intensity of rainfall (Chang et al., 2010), sea level rise (Hallegatte et al., 2011), and inefficiency of old infrastructures can further increase the frequency of urban flood disasters (Schubert and Sanders, 2012). Moreover, increasing the population and urbanization are leading to expand urban areas in the flood-prone areas, which magnifies the scale of damage caused by urban flooding (Neumann et al., 2015). The most damaging consequences of urban flooding can be contamination with sewage water, traffic jams, disruption of water and power supply, damage to transportation systems, infrastructure failure, injury, and loss of life (Jonkman and Vrijling, 2008).

Spatial modeling and mapping of the urban flood help the urban authorities to predict the spatial distribution of the flooding zones and its intensity. Therefore, decision-makers and authorities could develop effective flood prevention and management plans using a well-developed systematic framework and optimized models (Torres et al., 2014). Recently, several attempts have been made to analyze the interactions between urbanized areas and drainage infrastructures and the impact on surface runoff (Schmitt et al., 2004; Chen et al., 2009; Darabi et al., 2019). Progress in computational methods and availability of spatial data now permit more accurate modeling of the dynamic processes of flooding and urban flood prediction, mitigation, and risk management (Fewtrell et al., 2008).

Model optimization is vital when one 'optimum' solution needs to be identified among others (Marler and Arora, 2004) and it is especially important when analytical methods cannot solve the problem within the required time (Deb, 2012). For example, *meta*-heuristic algorithms can be combined to exploit their advantages and overcome their weaknesses, and thus obtain more accurate results (Yagiura and Ibaraki, 2001). Several attempts have been made to construct hybrid optimized models by utilizing different existing models, e.g., genetic algorithm (GA) and ant colony optimization (ACO) (Liu et al., 2017); simulated annealing (SA) and particle swarm optimization (PSO) (Javidrad and Nazari, 2017); SA and whale optimization algorithm (WOA) (Mafarja and Mirjalili, 2017); or PSO and grey wolf optimizer (GWO) (Şenel et al., 2019). These hybrid optimized models utilize the abilities of one algorithm to neutralize the deficiencies of another, e.g., the inability of GA for local searches can be solved by combining it with the bee algorithm (BA) (Şenel et al., 2019).

Artificial neural network (ANN) models have been utilized in different engineering fields due to the strength of neural networks in non-linearity and data-driven aspects. Beside of the well-documented advantages for using ANN (e.g. low cost of the model construction and flexible capability on input–output mapping for complex systems, which make it extensively used for prediction of dynamic variables such as geographical information), the main mentioned drawbacks of ANN are the large amounts of the training data required particularly for manners with many layers, extensive training time, high probability of over-fitting and difficulty of interpreting (Chen et al., 2020). Optimization of ANN is required to overcome its main shortcomings, which are lack of explanatory power in the trained networks due to their complex structure and over-fitting problems (Wen et al., 2019; Sessarego et al., 2020). Following the previous study (Darabi et al., 2019) and using data provided by Darabi et al., (2019), the aim of this study was to utilize and compare the four commonly used ML algorithms including random forest (RF), logistic model tree (LMT), classification, and regression trees (CART), J48 decision tree (J48DT) with new optimized ANN model for spatial prediction of urban flooding with the swarm intelligence-grey wolf (SGW) algorithm as a heuristic technique inspired by bird flocking, wolf pack hunting, and their social psychology (Le et al., 2009). This can be led to reduce the number of inputs to the ANN and select the most effective conditioning variables.

2. Study area

The study area is Sari city, located in Northern Iran (extended between 35°58′39″ to 36°50′12″ North and 52°56′42″ to 53°59′32″ East) where is characterized as lowland with altitude ranges between 9 and 82 m above sea level (a.s.l.)) (Fig. 1). The city occupies an area of approximately 42 km^2 and it is the second major city in the Mazandaran province (it is the capital of Mazandaran province) with a population of 296,417 according to the 2016 census. The city is characterized by built-up areas in the center, surrounded by agricultural land, small areas of orchards, and different types of natural environment. Mean annual precipitation in the region is 734 mm and mean annual temperature is 13.6 °C (Darabi et al., 2019). The city is located in the outlet of the Tajan basin (the city of Sari receives most of the surface runoff, by the rainy streams due to its location and is bordered by high mountains to the south of the Tajan River, passing through the eastern part of the city. In the recent years, one of the main causes of the flooding over the Sari city were river floods (Sharifinia, 2019). During each year prolonged heavy precipitation importantly created large volumes of surface runoff, which triggered a significantly the urban flood over the Sari city. In addition, the city of Sari is characterized as lowland and it has few drainage networks and most of them have been constructed for several years ago, which are old and have low capacity. Therefore, the surface runoff flow cannot be discharged in time when heavy precipitation occurs, which leads to serious water accumulation and make inundated areas (Abdi et al., 2019). Hydro-climate data for the present study were used from the Iranian Meteorological Organization (IRIMO) for Sari synoptic station.

3. Methodology

3.1. Urban flood locations (in situ analyses and sampling)

All available historical data on floods was used as auxiliary data (flood and non-flood locations during the several past flood events). Also, flood inventory data were obtained by historical and field surveys data which were conducted by Sari municipality and regional water company of Mazandaran to identify flooded areas and non-flooded areas during high-intensity precipitation. Table 1 shows the available historical database (2007–2016) and collected field survey databases (2017–2019) on floods. Two equal sets of points were identified randomly for both categories of flood and non-flood areas. Therefore, 113 locations for each category were recorded using a global positioning system (GPS) device. Each set is divided into training (70% of data − 79 points) and testing (30% of data – 34 points) groups. The flood locations were allocated by a value of 1 and non-flood locations were assigned by a value of 0. All historical database for flooded areas which were updated and employed in the current study, have been already used in the previous study by Darabi et al. (2019).

3.2. Conditioning variables in flood inundation mapping

Eight conditioning factors were tested in flood susceptibility mapping: elevation, slope, distance to channel, distance to river, land use/land cover, precipitation, curve number (CN), and depth to groundwater. All urban flood conditioning factors which used in this study, have been already applied in the previous study by Darabi et al. (2019).

Precipitation: Data on daily precipitation from meteorological for 16 stations in Mazandaran province (obtained from IRIMO for 1989–2018 period) were applied to extract a spatial rainfall map by applying the Kriging interpolation method in ArcGIS GIS 10.5. The mean

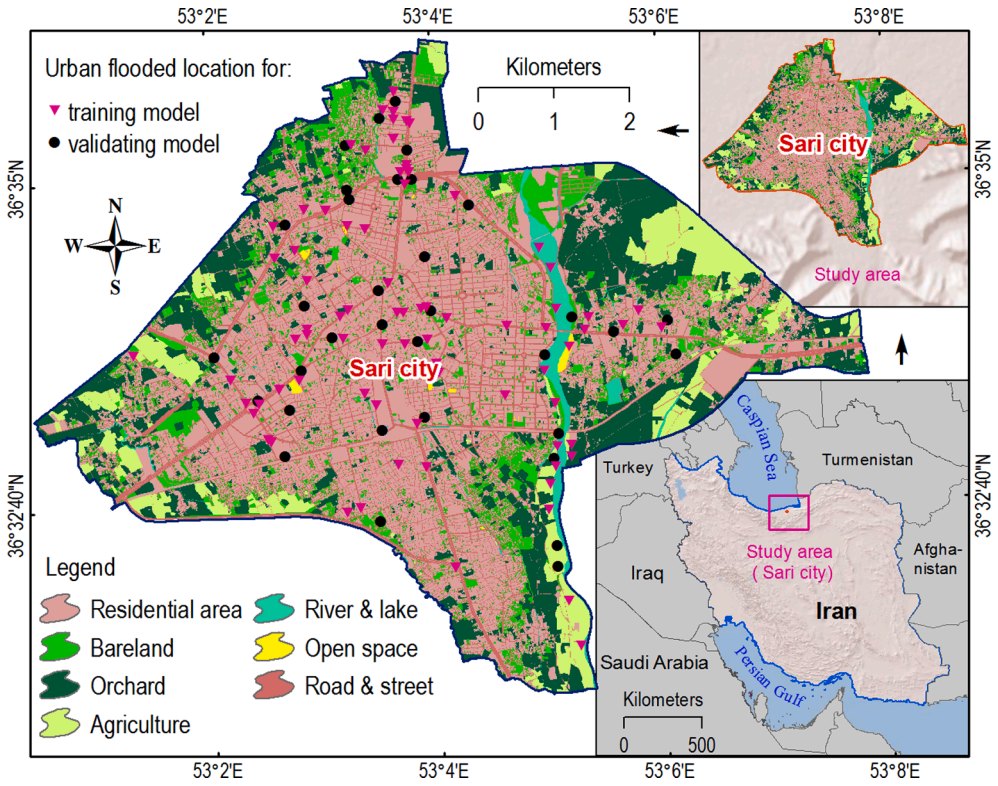

Fig. 1. Maps showing the layout of Sari city, flood locations used in training and validation of the model, and the position of the city in Northern Iran.

Table 1
Available historical database and collected field survey databases on floods.

	Row	Flood event	Precipitation (mm)
Data collected using available historical database on floods	1	2007.10.18	56
	2	2007.11.04	56
	3	2008.10.10	63
	4	2009.03.31	55
	5	2009.11.22	64
	6	2011.01.10	60
	7	2012.09.28	57
	8	2012.10.11	39
	9	2013.09.26	85.4
	10	2013.10.21	72
	11	2013.12.04	65
	12	2014.06.04	51.2
	13	2014.10.20	51.2
	14	2015.07.20	83
	15	2015.10.09	55.2
	16	2016.02.29	57
	17	2016.09.08	58
Data collected using field survey	18	2017.03.23	34.5
	19	2017.04.14	37
	20	2018.10.06	42.5
	21	2019.03.18	112.5
	22	2019.03.24	35

annual precipitation varied from 722 mm in the east to 745 mm in the west and northwest of the study area (Fig. 2a).

Land use/land cover: The land use/land cover map was obtained from Sari city authority (Darabi et al., 2019). Based on the land use data (Fig. 2b), seven categories of land cover were recognized: residential, road & street, open space, agricultural, bare land, orchard, and water body (river).

Digital elevation model (DEM): A DEM with 5 m resolution was prepared in ArcGIS 10.5 by applying the Kriging interpolation method of interpolation points (Fig. 2c). The attitude of the Sari city ranges from 9 m asl in the north and northeast to 82 m asl in the south. The database of the elevation was obtained from Sari municipality.

Slope: Slope percent plays an important role in flood susceptibility, as it affects runoff velocity and intensity of flow. A slope percent map (5 m) was prepared using the DEM in ArcGIS 10.5. Slope percent was divided into four classes: <2%, 2–4%, 4–6%, and > 6%, based on the classification used by Sari city authority (Fig. 2d).

Curve number (CN): Curve number is a function based on hydrological conditions and land use/land cover, soil type, and moisture, which was first developed by USCS or United States Soil Conservation Service. Land use/land cover and hydrological soil group (HSG) maps of the Sari city were used to prepare a CN map in ArcGIS 10.5 (Fig. 2e), by the ArcCN-runoff tool (Darabi et al., 2019).

Distance to river: Distance to river has an important role in flood-prone areas in riversides. Distance to the Tajan River, which passes through the east of Sari city, was extracted using the Euclidean distance module in ArcGIS 10.5 (Fig. 2f).

Distance to channel: Surface water is collected by urban channels, which should have sufficient capacity to drain all surface water from the city. The channels in Sari city do not have such capacity, so it is very important to consider distance to channels as a flood conditioning factor. Distance to channel was extracted using the Euclidean distance module in ArcGIS 10.5 (Fig. 2g).

Depth to groundwater: In urban areas, depth to groundwater level significantly affects surface water runoff (Howard and Gerber, 2018). In this study, depth to groundwater data were obtained from the IRIMO and groundwater level map were extracted from 28 piezometric wells by the interpolation method by integrated distance weighting (IDW) in ArcGIS 10.5 (Fig. 2h).

3.3. Machine learning (ML) algorithms

Machine learning (ML) aims to develop methods and algorithms to learn and forecast data. ML algorithms are important for several reasons, e.g., they can i) handle complex systems with huge data, ii) solve

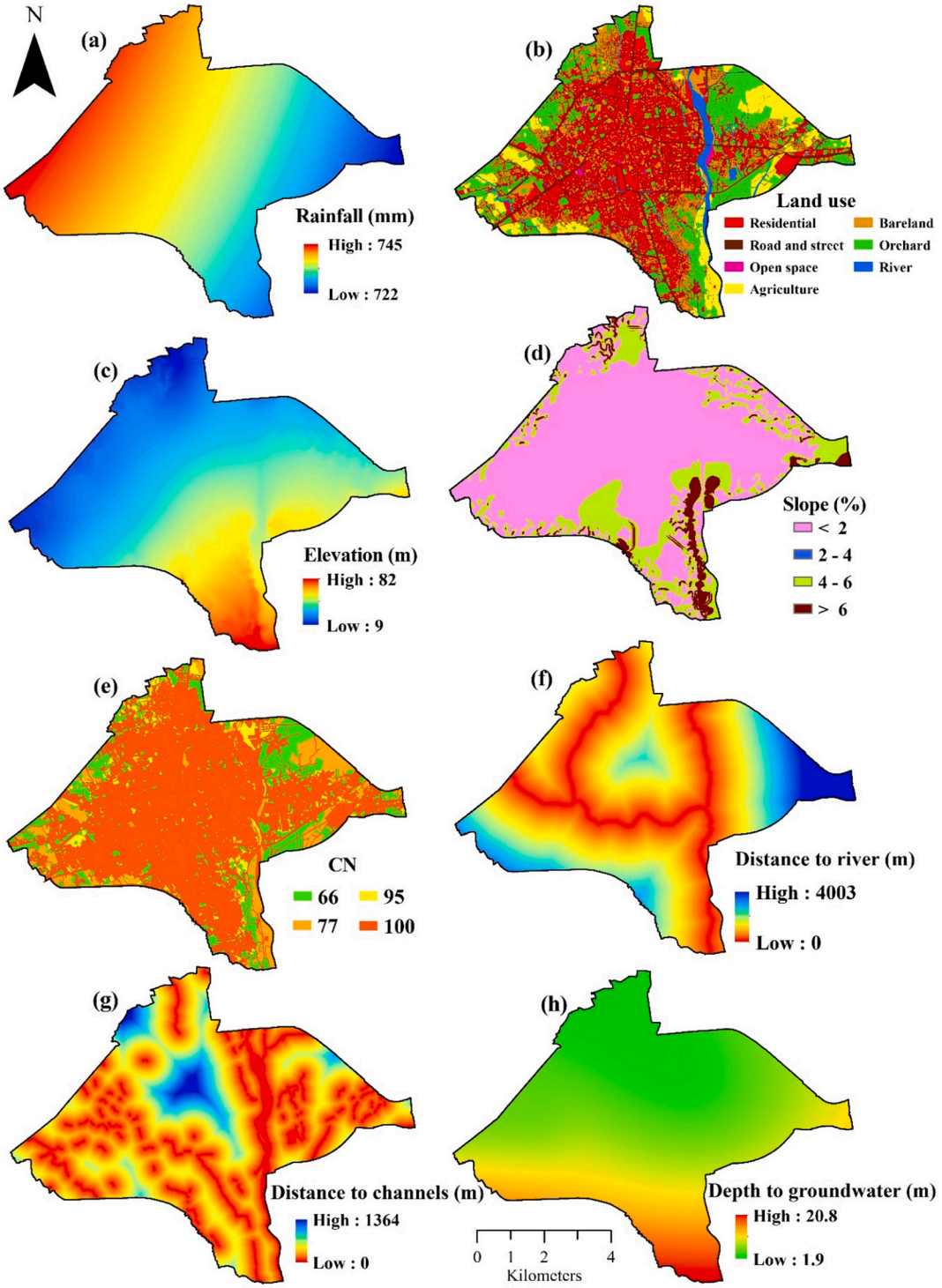

Fig. 2. Maps showing possible conditioning factors for urban flood inundation in Sari city: a) Rainfall, b) land use, c) elevation, d) slope, e) curve number (CN), f) distance to river, g) distance to channel, and h) depth to groundwater.

specialized problems by specialized ML methods, iii) be used for forecasting and classification purposes, and iv) be applied to describe the performance of the data input with respect to historical data records (Demolli et al., 2019). In this study, four commonly used ML algorithms including random forest (RF), logistic model tree (LMT), classification, and regression trees (CART), J48 decision tree (J48DT) were employed as standard or benchmark models for judging the performance of the novel hybridized model.

3.3.1. *Random forest (RF)*

The concept of random forest (RF) was first proposed by Ho (1998) and extended by Breiman (2001). RF as a powerful ensemble ML algorithm was developed by the combination of regression and classification methods and statistical theory (Tan et al., 2020). It can be employed for many predicted trends and the average prediction of decision trees (Xing et al., 2019). The RF algorithm has been employed in different fields, such as land-cover classification using remote sensing data and flood risk and hazard mapping (Zhao et al., 2018). The algorithm has two main

advantages that improve the accuracy of prediction: i) its ability to handle huge datasets with a nonparametric and robust method and correlated conditional variables; and ii) its capacity for variable importance assessments using a random arrangement of the variables, by comparison and evaluation of each variable in the prediction results for its importance (Zhao et al., 2018).

3.3.2. J48 Decision tree (J48DT)

J48 decision tree (J48DT) is a new classification tree-based technique that has been employed in only a few studies. Predictive ability of the algorithm has been assessed and validated in a previous study using statistical and receiver operating characteristic (ROC) curve methods (Pham et al., 2017). For binary classification variables (here flood or non-flood locations), J48DT creates a tree, which includes a root node and internal branch and leaf nodes. The root node consists of the input dataset, the internal branch nodes relate to the decision function, and the leaf nodes indicate the production of a specified contribution of the dataset. Compared with other decision tree models, J48DT is considered best in terms of classification accuracy, which is trained in two steps: i) building, and ii) pruning the classification tree (Zhao and Zhang, 2008).

3.3.3. Classification and regression tree (CART)

Classification and regression tree (CART) is a recursive partitioning algorithm that used to predict continuous dependent and categorical predictor conditioning factors (Zhao et al., 2016). CART, which was proposed for the first time by Breiman et al. (1984), has gained in popularity during recent years. However, because of overfitting and high sensitivity of CART to minor changes in all training input data, it is viewed as an unstable ML algorithm (Erdal and Karakurt, 2013).

3.3.4. Logistic model tree (LMT)

Logistic model tree (LMT), a ML algorithm suggested by Landwehr et al. (2003), is a hybrid classification model combining logistic regression (LR) with decision tree (DT) functions, which can boost the precision of prediction (Chen et al., 2017). In LMT, variable splitting is performed with the maximum information ratio obtained. For splitting categorical and numerical variables with *c* specific values, the node has *c* child nodes and two child nodes, respectively (Lee and Jun, 2018). For pruning the nodes of the tree, the LMT algorithm employs a Logit Boost function to set up the logistic regression method, and it uses cross-validation to discover multiple Logit Boost iterations to stop overfitting of all training input data (Arabameri et al., 2020).

3.3.5. Artificial neural network (ANN) models

Neural network models are a set of *meta*-heuristic population-based optimization algorithms. Computational NN models have been broadly employed in different scientific fields, for prediction purposes in most cases (Madsen et al., 2017; Zhang et al., 2020). The ANN model has strong self-learning, self-compatibility, fitness, error tolerance, and extension capabilities, inspired by biological nervous systems. It shows high performance in fitting multivariate analysis by better learning efficiency (Zhao et al., 2019). The purpose of ANN model optimization is to get an optimum solution (Shirwaikar et al., 2019). Within the data mining field, the ANN algorithm has been used to solve many practical problems. In this study, it was used for urban flood susceptibility mapping.

3.3.6. Swarm intelligence algorithm

The swarm intelligence algorithm is one of the major popular optimization models applied by researchers in different subfields (Arani et al., 2013; Yang, 2014). During recent years, the swarm intelligence algorithm has been used to imitate behavior in nature (Şenel et al., 2019), e.g., to understand crowd behavior in biological systems (Qasim, and Bhatti, 2019). It is one of a family of nature-inspired modeling approaches based on the collective behavior of social swarms in nature (e.g., honeybees, ant colonies, birds, fish). However, the swarm intelligence algorithm seeks to identify an optimal result from the social actions of many individuals (Mosa et al., 2019), according to the premise that individuals' interactions lead to intelligent behaviors at group level (Zedadra et al., 2018). It comprises three steps: i) Initialize the swarm of predictor variables as dimensional space, ii) set parameters of the swarm algorithm (e.g., maximum iteration and population); and iii) predict a robustness value and randomly determine the primary best situation (Bui et al., 2019).

3.3.7. Grey wolf optimizer (GWO)

Grey wolf optimizer is a novel bionic, population-based, and heuristic optimization algorithm that forms a pyramid with the most influential wolf at the remaining wolves in descendant importance in lower situations (Bui et al., 2019). GWO was developed by Mirjalili et al. (2014) according to the social hunting nature of grey wolves. It mathematically mimics the social leadership hierarchy and hunting behavior based on the grey wolves working together to detention prey with a clear cooperation. The GWO algorithm for predation is divided into three stages: encircling, hunting, and attacking (Long, 2016; Niu et al., 2019). GWO, with its low number of parameters and ease of implementation, has faster evolutionary programming and faster convergence than the swarm intelligence algorithm (Daniel et al., 2017). GWO was effectively applied in a forest fire research by Bui et al. (2019). Search agents (wolves) in GWO, as swarm-based algorithms, are arbitrarily situated in the d-dimensional space. After each iteration, the positioned and fitness values of wolves/search agents are updated. The optimal solution to the problem at hand is the final location of the top wolf (Bui et al., 2019).

3.4. Designing and proposing a neural network model optimized by swarm intelligence and grey wolf algorithms (ANN-SGW)

Optimization of models is important to achieve an optimum solution in a complicated d-dimensional space. When the problem-solving needs too much time, optimized approaches can help, however, an overall optimized algorithm is not guaranteed (Şenel et al., 2019). Optimization is also a crucial activity in model design, allowing programmers and planners to produce better designs, which can save time and costs. Many optimization problems in engineering are complex and difficult to solve with conventional optimization models, such as mathematical programming. By hybridizing a model with different algorithms, it is possible to combine the advantages of the algorithms and produce a better-optimized model (Cui and Bai, 2019; Jia et al., 2019). In this study, an ANN model was optimized using novel optimizer algorithms (swarm intelligence and GWO) in a parallel computing approach, to improve spatial prediction of urban inundation susceptibility. The optimized model (ANN-SGW) was used to recognize the most flood-prone areas in the study city, compared with actual data. The proposed ANN-SGW model has a simple construction, with a low number of factors and simulations, avoiding the complexity of large-scale networks, and combines the advantages of swarm intelligence and GWO with those of ANN.

3.5. Loss function and optimization algorithm

The ANN model was first generated for spatial prediction of urban flooding, and then optimized using the SGW algorithms. The purpose of optimization was to search and identify the best weights of the model, in which the difference between flood inventory data and predicted flood locations is minimized. The difference was determined using a loss function (LoF), designed as follows (Bui et al., 2019):

$$\mathrm{LoF} = \sum_{1}^{n} \frac{(\mathrm{Pred}_i - \mathrm{Tag}_i)}{\mathrm{n}} \tag{1}$$

where $\mathrm{Pred_i}$ is predicted flood in the ANN model output; $\mathrm{Tag_i}$ is the actual flood measured value; and n is the number of total flood locations

used.

Parameters used in the SGW algorithm were G0 = 100, α = 20, ω = 0.5, c1 = 1, c2 = 3, and population size = 5 as suggested by Jayaprakasam et al. (2015). The training process was run for 200 iterations.

3.6. Model assessment and benchmark model comparison

In statistical analysis of data mining techniques, a known error matrix is the confusion matrix, which allows the performance of supervised models to be assessed. Here we used nine different cutoff-dependent metrics from the confusion matrix, namely: true positive and negative (TP and TN), false positive and false negative (FP and FN), positive and negative predictive values (PPV and NPV), sensitivity, specificity, and efficiency. The four elements of the confusion matrix are TP, TN, FP and FN (Frattini et al., 2010). Sensitivity (true positive rate (TPR), see equation (2)), specificity (false positive rate (FPR), see equation (3)), and efficiency (E, equation (4)) determine the proportion of actual flooded locations that are accurately identified. The other cutoff-dependent metrics used, PPV and NPV, are the ratio of positive and negative results, respectively, in statistical analysis (equations (5) and (6)), and thus explain model performance by applying primary statistical criteria (TP and TN) in the confusion matrix (Fletcher et al., 2018). Using the PMT tool, all cutoff-dependent metrics used for model performance assessment were applied (Rahmati et al., 2019). Area under the curve receiver operating characteristic curve (AUC-ROC), a cutoff-independent metric, was also used (equation (7)), as it is effective in organizing models and assessing their performance visually (Fawcett, 2006). It is known as a decisive metric where values closer to 100% indicate better performance of a model (Pontius and Schneider, 2001).

$$\text{Sensitivity} = \tag{2}$$

$$\text{Specificity} = \frac{FP}{FP + TN} \tag{3}$$

$$Efficiency = \frac{TP + TN}{TP + TN + FP + FN} \tag{4}$$

$$PPV = \frac{TP}{TP + FP} \tag{5}$$

$$NPV = \frac{TN}{TN + FN} \tag{6}$$

$$AUC = \int_0^1 f(FPR)dFPR = 1 - \int_0^1 f(TPR)dTPR \tag{7}$$

4. Results

4.1. Training the ANN-SGW model and performance assessment

The results for goodness-of-fit of the ANN-SGW model are shown in Table 2. Among the cutoff-dependent evaluation metrics, the value obtained for PPV, NPV, sensitivity, specificity, and efficiency in the training step was 93.7%, 87.3%, 88.1%, 93.2%, and 90.5%, respectively. The results of the confusion matrix criteria indicate a considerable arrangement between the trained model and observed dataset. AUC, a cutoff-independent metric, had a value of 96.3% in this step, reflecting high fitting skill of the ANN-SGW model. There was therefore agreement between the cutoff-dependent and -independent metrics as regards performance of the model. However, goodness-of-fit individually estimates how well the model fits the training dataset and cannot be used for determining the ability of the model in prediction (Tehrany et al., 2015). A testing step is needed to determine the predictive performance. In the validation step, the ANN-SGW model showed considerably maximum predictive performance based on both the cutoff-independent metrics (PPV = 85.3%, NPV = 73.5%, sensitivity = 76.3%, specificity = 83.3%, efficiency = 79.4%) and the cutoff-independent metric (AUC = 88.2%) and evaluation criteria (Table 2, Fig. 3). The validation results obviously demonstrated robust arrangement between observed values (i.e., reference data) and predicted values by the ANN-SGW model. Following Rahmati et al. (2020), the predictive performance of ANN-SGW can be classified as very good (80% < AUC < 90%).

Table 2
Performance of the hybridized neural network-swarm intelligence-grey wolf algorithm (ANN-SGW) model in the training and validation steps

Evaluation approach	Evaluation metric	Goodness-of-fit	Predictive performance
Cutoff-dependent	True positive, TP	74	29
	True negative, TN	69	25
	False positive, FP	5	5
	False negative, FN	10	9
	Positive predictive value (PPV, %)	93.7	85.3
	Negative predictive value (NPV, %)	87.3	73.5
	Sensitivity (%)	88.1	76.3
	Specificity (%)	93.2	83.3
	Efficiency (%)	90.5	79.4
Cutoff-independent	Area under receiver operating curve (AUC, %)	96.3	88.2

4.2. Comparison of the ANN-SGW model with benchmark models

To confirm the performance of the ANN-SGW model, its predictive ability was compared with that of four commonly used benchmark models (RF, LMT, CART, J48DT). Among these, RF showed the highest accuracy in the training step in terms of both the cutoff-dependent (PPV = 87.3%, NPV = 72.2%, sensitivity = 75.8%, specificity = 85.1%, efficiency = 79.7%) and cutoff-independent (AUC = 89.4%) evaluation metrics (Table 3). It was followed by LMT (PPV = 84.8%, NPV = 69.6%, sensitivity = 73.6%, specificity = 82.1%, efficiency = 77.2%, AUC = 80%), and then J48DT (PPV = 87.3%, NPV = 63.3%, sensitivity = 70.4%, specificity = 83.3%, efficiency = 75.3%, AUC = 72.9%), and CART (PPV = 77.2%, NPV = 67.1%, sensitivity = 70.1%, specificity = 74.6%, efficiency = 72.1%, AUC = 72.2%). Therefore, agreement was obtained between observed values and values predicted by the benchmark models in the training step. Importantly, comparison of all results indicated that the ANN-SGW model had the highest goodness-of-fit, followed by RF, LMT, J48DT, and CART.

The validation results for the benchmark models are shown in

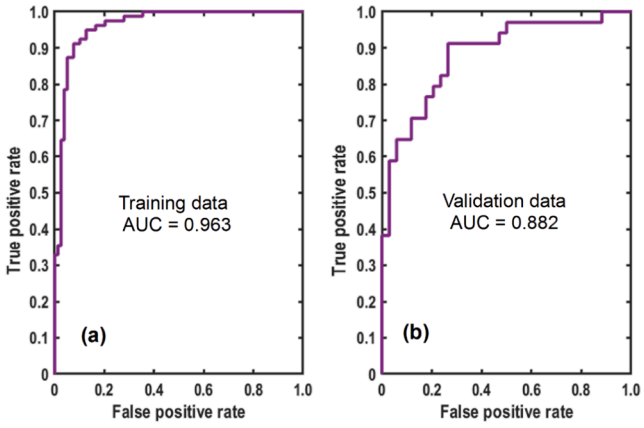

Fig. 3. Receiver operating curve (ROC) and area under receiver operating curve (AUC) of the hybridized neural network-swarm intelligence-grey wolf algorithm (ANN-SGW) model with (left) the training dataset and (right) the validation dataset.

Table 3
Goodness-of-fit of the benchmark models (random forest (RF), J48 decision tree (J48DT), classification and regression trees (CART), logistic model tree (LMT)) in the training step

Evaluation metric	RF	J48DT	CART	LMT
True positive, TP	69	69	61	67
True negative, TN	57	50	53	55
False positive, FP	10	10	18	12
False negative, FN	22	29	26	24
Positive predictive value (PPV, %)	87.3	87.3	77.2	84.8
Negative predictive value (NPV, %)	72.2	63.3	67.1	69.6
Sensitivity (%)	75.8	70.4	70.1	73.6
Specificity (%)	85.1	83.3	74.6	82.1
Efficiency (%)	79.7	75.3	72.1	77.2
Area under receiver operating curve (AUC, %)	89.4	72.9	72.2	80.0

Table 4
Predictive performance of the benchmark models (random forest (RF), J48 decision tree (J48DT), classification and regression trees (CART), logistic model tree (LMT)) in the validation step

Evaluation metric	RF	J48DT	CART	LMT
True positive, TP	32	32	29	31
True negative, TN	20	16	20	19
False positive, FP	2	2	5	3
False negative, FN	14	18	14	15
Positive predictive value (PPV, %)	94.12	94.12	85.29	91.18
Negative predictive value (NPV, %)	58.82	47.06	58.82	55.88
Sensitivity (%)	69.57	64.00	67.44	67.39
Specificity (%)	90.91	88.89	80.00	86.36
Efficiency (%)	76.47	70.59	72.06	73.53
Area under receiver operating curve (AUC, %)	88.1	69.7	69.8	75.6

Table 4 and Fig. 4. Again, RF outperformed the other benchmark models based on cutoff-dependent (PPV = 94.12%, NPV = 58.82%, sensitivity = 69.57%, specificity = 90.91%, efficiency = 76.47%) and cutoff-independent (AUC = 88.1%) evaluation metrics. It was followed by LMT (PPV = 91.18%, NPV = 55.88%, sensitivity = 67.39%, specificity = 86.39%, efficiency = 73.53%, AUC = 75.6%), and then CART (AUC = 69.8%) and J48DT (AUC = 69.7%). Therefore, the proposed ANN-SGW model (AUC = 88.2%) had higher predictive performance than all benchmark models based on both cutoff-dependent and independent assessment metrics.

4.3. Variable importance

Since the ANN-SGW model showed the highest accuracy in both the training and testing dataset, importance of the variable has been calculated by the ANN-SGW model. Fig. 5 illustrates the relative importance (RI) of predictor variables in spatial modeling of urban flood susceptibility. Distance from channel, distance from river, and depth to groundwater had the greatest importance in urban inundation, with RI equal to 31%, 22%, and 19%, respectively. They were followed by precipitation (RI = 11%), land use (RI = 10%), and curve number (RI = 7%).

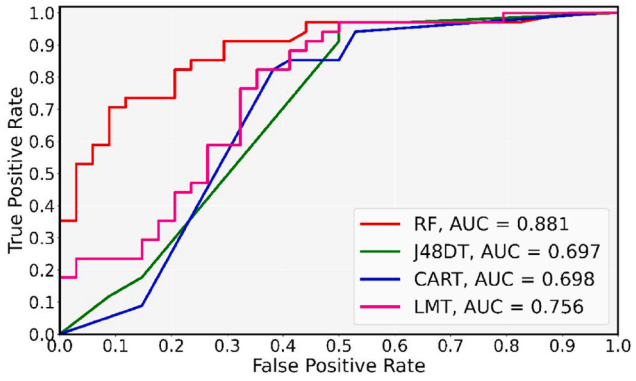

Fig. 4. Receiver operating curve (ROC) and area under receiver operating curve (AUC) of the four benchmark models (random forest (RF), J48 decision tree (J48DT), classification and regression trees (CART), logistic model tree (LMT)) in the validation step.

4.4. Urban inundation susceptibility mapping

The urban flood inundation maps were generated by the ANN-SGW and benchmark models are shown in Fig. 6 and Fig. 7. Upon preliminary review, distribution of high flood susceptibility zones seemed to be clearly distinguished over the Sari city. Especially, all the proposed ANN-SGW and benchmark models revealed a comparatively similar pattern of flood susceptibility in the Sari city (Fig. 6 and Fig. 7). Central, northern, western, and southwestern parts of Sari city fell under highly flood-susceptible areas, while eastern, southern, and southeastern parts showed significantly fewer flood susceptibility zones.

5. Discussion

5.1. Urban flood mapping approaches

Flood prediction in urban environments is important for urban planners and policymakers, in order to reduce susceptibility to future floods (Kim et al., 2015). Different methodologies for urban flood assessment were considered and discussed by previous researchers using probabilistic and deterministic approaches (Di Baldassarre et al., 2009), high resolution of topographic modeling (Abily et al., 2016), hydrodynamic numerical modeling (Glenis et al., 2018; Costabile et al., 2020; Dong et al., 2021). Recently numerous works have been conducted to improve the predictive capacity of the one-dimensional urban flood modeling, but so far it is noticeable that these attempts are still far from a satisfactory application of these models in urban flood prediction. For example, Eini et al., (2020) assessed the hazard and vulnerability of urban flood using Maximum Entropy (MaxEnt) and Genetic Algorithm Rule-Set Production (GARP) algorithms that have been used by previous researchers (Darabi et al., 2019) without any optimization and hybridization. While Andaryani et al., (2021) evaluated the prediction ability of artificial neural network (ANN) algorithms as a one-dimensional flood modelling coupled with hard and soft supervised classification algorithms using three multi-layer perceptron (MLP), fuzzy adaptive resonance theory (FART), self-organizing map (SOM) algorithms with

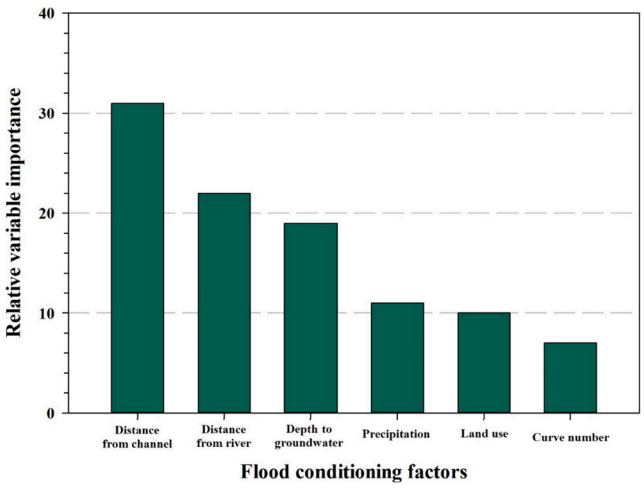

Fig. 5. Relative variable importance of the six most important flood conditioning factors tested, based on the hybridized neural network-swarm intelligence-grey wolf algorithm (ANN-SGW) model.

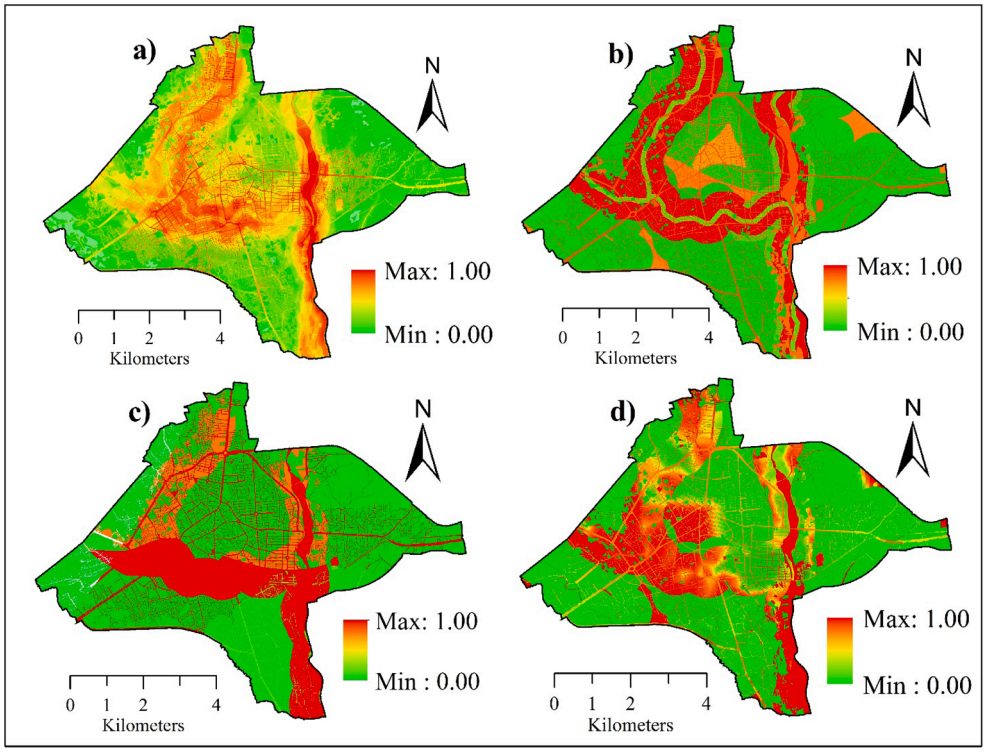

Fig. 6. Urban flood susceptibility maps produced by a) the random forest; b) the J48 decision tree; c) the classification and regression trees (CART); and d) the logistic model tree LMT models.

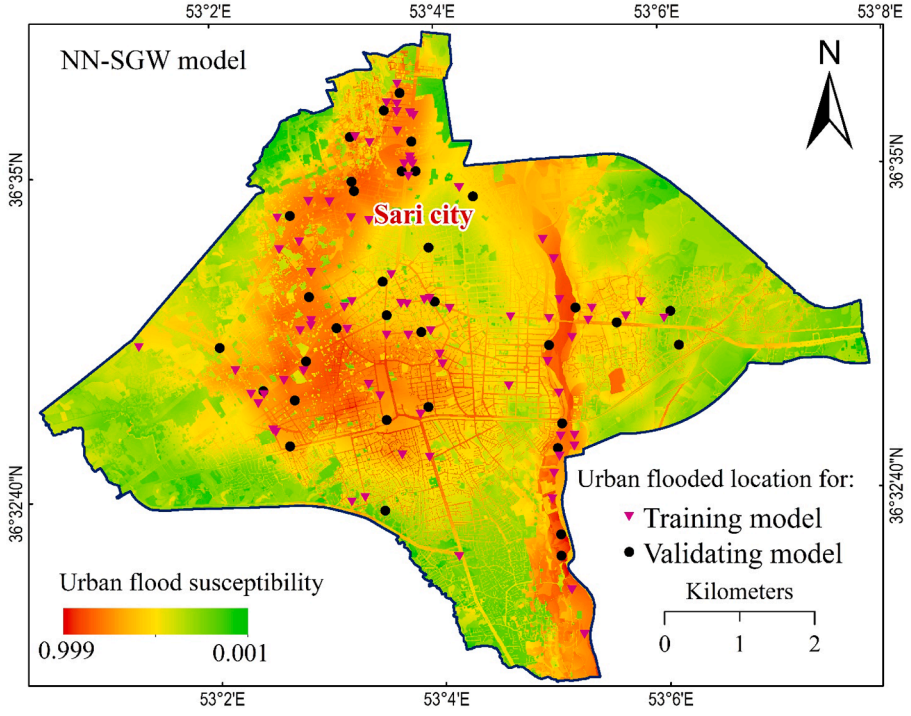

Fig. 7. Urban flood susceptibility maps produced by the hybridized neural network-swarm intelligence-grey wolf algorithm (ANN-SGW) model.

different activation functions of sigmoidal, linear, commitment, typicality. MLP-S and MLP-L had slightly higher accuracy and less time-consuming. Despite the contribution of these studies to the science of flood modelling, their main issue was to optimize the ML algorithms, which can be accompanied by urban flood modelling and highlight uncertainty of flood mapping in one dimension. In this study, ML techniques in the field of urban flood inundation modelling are applied to facilitate the critical discussion over Sari city. Specifically, different flood susceptibility maps were extracted for the study area. The flood susceptibility maps were derived by applying RF, J48DT, CART, and LMT models. The derived urban flood maps were then compared to the novel hybridized ANN-SGW (as fifth map) and the pros and cons of the

above-mentioned ML algorithms were discussed below.

5.2. Comparing flood susceptibility maps

A novel hybridized ANN-SGW model for spatial prediction of urban flooding was developed in this study, and the resulting map was compared, based on different statistical evaluation criteria, with maps produced by benchmark models. The results demonstrated that the ANN-SGW model had an excellent performance in flood-prone prediction. Artificial ANN models have a powerful ability to predict flood susceptibility, as confirmed previously by Falah et al. (2019). Importantly, excellent performance of the RF and LMT models in flood susceptibility mapping has been demonstrated previously, resulting in strong recommendations for their use as best available models (Lee et al., 2017). Pourghasemi et al. (2020) demonstrated that, in addition to showing outstanding performance in predicting flood susceptibility, the RF model can also be used for multi-hazard modeling at a regional scale. However, the results obtained in the present study showed that our novel ANN-SGW model outperformed RF and other benchmark models. In general, the SGW *meta*-heuristic algorithm enhances the standalone ANN model by narrowing the deviation between predicted and actual values. According to the literature, the ANN model has some problems, such as poor generalization ability for unseen data, weaker scalability when using several variable types, and it needs training to operate and often requires numerous recalibrations (Piotrowski and Napiorkowski, 2013; Ahmad et al., 2014). In this study, the SGW algorithm overcame these challenges and the ANN-SGW model revealed excellent performance, computational and robustness speed, as found previously for the GWO algorithm by Komaki and Kayvanfar (2015). Guha et al. (2016) also found GWO to be useful in enhancing model performance. GWO is a novel nature-inspired metaheuristic swarm intelligent algorithm, and it needs low number of parameters and ease of implementation, faster evolutionary programming and quicker convergence than the other swarm intelligence algorithms such as Particle Swarm Optimization (PSO), Firefly Algorithm (FA), Bat Algorithm (BA), Cuckoo Search (CS), Ant Colony Optimization (ACO), Artificial Bee Colony (ABC) and many other algorithms, which are recently added to swarm intelligent algorithms are Salp Swarm Algorithm (SSA), Moth-flame Optimization (MFO), Harris Hawks Optimization (HHO), Squirrel Search (SS), and Whale Optimization Algorithm (WOA) (Gupta and Deep, 2020). It has received lots of interest from the heuristic algorithm community for its superior optimization capacity. It is also easy to trap into the local optimum when solving complex and multimodal functions. GWO has shown potential to solve several real-life applications and it was effectively applied in different research areas such as forest fire by Bui et al., (2019); water resource system over the irrigation areas (support vector machine model was optimized based on the GWO (GWO-SVM)) by Liu et al. (2020); for optimization of water resources allocation in transboundary river basins by Yu and Lu, (2018). Also, it has been successfully applied into various global optimization requirements due to its advantage of few control parameters in economic studies (Jayabarathi et al., 2016), landslide susceptibility modeling (Panahi et al., 2020), feature selection (Hu et al., 2020), groundwater contamination and remediation (Majumder and Eldho, 2020), and streamflow prediction (Tikhamarine et al., 2020). Bui et al. (2019) developed a hybridized model based on swarm intelligence model for flood mapping and found that the swarm intelligence algorithm enhanced the predictive skill of the model. Our novel model can construct a valid flood susceptibility map for urban areas where a hydraulic dataset is lacking. It can thus assist in robust flood contingency planning for urban areas. Importantly, for urban areas where flooding presents a pressing challenge, the proposed model can be utilized to protect main applied scopes of social and environmental.

5.3. Variable importance

Credible information of the relationship between target variables, i.e., urban flood events and predictor variables, can help decision-makers, but these relations are still rather complex and poorly evaluated (Feng et al., 2015). This study tried to bridge this research gap. The ANN-SGW model, which had the highest accuracy of all models tested in this study, demonstrated that distance from channel, distance from river, and depth to groundwater were the most important variables for spatial prediction of flood susceptibility in Sari city. This is useful information for urban planning studies and resolves the problematic of data scarcity by allowing the analyst to focus on important predictor variables (Ahmadisharaf et al., 2016). The results are consistent with our previous finding, obtained using Genetic Algorithm Rule-Set Production (GARP), that distance from channel and distance from river had the highest importance in urban flood inundation (Darabi et al., 2019). Similarly, Fernández and Lutz (2010) found distance from channel had greatest importance in spatial modeling of flooding in urban areas, while Ouma and Tateishi (2014) found that distance to drainage system is the main factor in urban flooding. However, according to Bui et al. (2019), the relative importance of variables for a flood modelling is generally has been influenced by the model structure, such that predictor variables making a large influence in a model might provide less information for another, and vice versa. For instance, in the present study and in a previous study by Fernández and Lutz (2010), CN (determined by cover type) was the least important predictor variable, whereas in our previous study with the GARP model CN provided useful information for urban flood modeling (Darabi et al., 2019). It worth mentioning that the dynamic of the conditioning variables in flood inundation mapping leads to different results over time (e.g. precipitation and depth to groundwater).

6. Conclusions

Floods have great threats to communities and its property, specifically in densely populated urban areas, where increasing the impermeable surfaces leads to intensify floods by increasing surface runoff. Since in developing countries hydraulic and hydrological data are not available over the urban environments and lack of required data is the main issue in urban flood modeling. This study set out to develop a robust hybridized model for spatial prediction of urban flood inundation as inspiration and insight for future studies and plans in next urban flood monitoring and mitigation strategies. Also, urban flood inundation identifies the most vulnerable areas based on physical characteristics that determine the propensity for flooding, it is an important element of flood mitigation and prevention strategies. A novel hybridized model (ANN-SGW) was developed and evaluated using statistical evaluation metrics and compared with several benchmark machine learning models. The degree of importance of topographic-environmental variables was evaluated using the ANN-SGW model. This work can serve as a basis for future studies seeking to predict flood susceptibility in urban areas using hybridized machine learning models and can also be applied in other urban areas where flood inundation presents a pressing challenge. Also, the results of this study can help decision-makers attendant investments out of dangerous zones (e.g. Riverian zone), save property and lives, as well as guarantee that investments consider flood events in urban environments with high-density population as well as multiple infrastructure (such as hospitals, schools and service networks). Our novel hybridized model is an important scientific contribution to development of a powerful model for spatial prediction of flooding in urban environments and the main conclusions of current study can be summarized as:

- The ANN-SGW model achieved strong predictive capacities outperforming all four benchmark models tested.

- The presented ANN-SGW model is recommended to use by local and regional municipality agencies to identify flood-prone areas and plan to mitigate future flood events.
- The analysis presented in this study provides a valuable screening of urban areas and can easily be modified to incorporate other conditions with other spatio-temporal resolutions.
- Since the simplicity of flood models is a primary purpose, the employed approaches in the current study were not sophisticated with regard to required model and availability of input data, therefore it can effortlessly be employed in other areas.

CRediT authorship contribution statement

Hamid Darabi: Conceptualization, Formal analysis, Investigation, Funding acquisition, Data acquisition, Methodology, Software, Writing – original draft, Writing – review & editing, Project administration. **Ali Torabi Haghighi:** Supervision, Writing – review & editing. **Omid Rahmati:** Conceptualization, Methodology, Software, Writing – original draft, Writing – review & editing. **Abolfazl Jalali Shahrood:** Writing – original draft, Writing – review & editing. **Sajad Rouzbeh:** Data acquisition. **Biswajeet Pradhan:** Writing – review & editing. **Dieu Tien Bui:** Conceptualization, Methodology, Software, Writing – review & editing.

Declaration of Competing Interest

The authors declare that they have no known competing financial interests or personal relationships that could have appeared to influence the work reported in this paper.

Acknowledgment

This work was supported by the Maa- ja vesitekniikan tuki r.y. (MVTT), to which the authors would like to express their deep gratitude and authors would like to thank Sari municipality and regional water company of Mazandaran for providing relevant data.

References

Abdi, K., Kamyabi, S., Zand Moghaddam, M.R., 2019. Integrated Assessment of Vulnerability, Resiliency and Space Risk against Flood in Sari. Physical Geography Res. Quarterly 51 (3), 431–445.
Abily, M., Bertrand, N., Delestre, O., Gourbesville, P., Duluc, C.M., 2016. Spatial Global Sensitivity Analysis of High Resolution classified topographic data use in 2D urban flood modelling. Environ. Modell. Software 77, 183–195.
Ahmad, A.S., Hassan, M.Y., Abdullah, M.P., Rahman, H.A., Hussin, F., Abdullah, H., Saidur, R., 2014. A review on applications of ANN and SVM for building electrical energy consumption forecasting. Renew. Sustain. Energy Rev. 33, 102–109.
Ahmadisharaf, E., Tajrishy, M., Alamdari, N., 2016. Integrating flood hazard into site selection of detention basins using spatial multi-criteria decision-making. J. Environ. Plann. Manage. 59 (8), 1397–1417.
Andaryani, S., Nourani, V., Haghighi, A.T., Keesstra, S., 2021. Integration of hard and soft supervised machine learning for flood susceptibility mapping. J. Environ. Manage. 291, 112731.
Arabameri, A., Chen, W., Loche, M., Zhao, X., Li, Y., Lombardo, L., Cerda, A., Pradhan, B., Bui, D.T., 2020. Comparison of machine learning models for gully erosion susceptibility mapping. Geosci. Front. 11 (5), 1609–1620.
Arani, B.O., Mirzabeygi, P., Panahi, M.S., 2013. An improved PSO algorithm with a territorial diversity-preserving scheme and enhanced exploration–exploitation balance. Swarm Evol. Comput. 11, 1–15.
Ashley, S.T., Ashley, W.S., 2008. Flood fatalities in the United States. J. Appl. Meteorology Climatology 47 (3), 805–818.
Breiman, L., 2001. Random forests. Mach. Learn. 45 (1), 5–32.
Breiman, L., Friedman, J., Olshen, R., Stone, C., 1984. Classification and regression trees. Wadsworth International Group 37 (15), 237–251.
Bui, D.T., Ngo, P.T.T., Pham, T.D., Jaafari, A., Minh, N.Q., Hoa, P.V., Samui, P., 2019. A novel hybrid approach based on a swarm intelligence optimized extreme learning machine for flash flood susceptibility mapping. Catena 179, 184–196.
Chang, H., Lafrenz, M., Jung, I.W., Figliozzi, M., Platman, D., Pederson, C., 2010. Potential impacts of climate change on flood-induced travel disruptions: a case study of Portland, Oregon, USA. Ann. Assoc. Am. Geogr. 100 (4), 938–952.
Chen, J., Hill, A.A., Urbano, L.D., 2009. A GIS-based model for urban flood inundation. J. Hydrol. 373 (1–2), 184–192.
Chen, S., Ren, Y., Friedrich, D., Yu, Z., Yu, J., 2020. Sensitivity analysis to reduce duplicated features in ANN training for district heat demand prediction. Energy and AI 2, 100028.
Chen, W., Xie, X., Wang, J., Pradhan, B., Hong, H., Bui, D.T., Duan, Z., Ma, J., 2017. A comparative study of logistic model tree, random forest, and classification and regression tree models for spatial prediction of landslide susceptibility. Catena 151, 147–160.
Costabile, P., Costanzo, C., De Lorenzo, G., Macchione, F., 2020. Is local flood hazard assessment in urban areas significantly influenced by the physical complexity of the hydrodynamic inundation model? J. Hydrol. 580, 124231. https://doi.org/10.1016/j.jhydrol.2019.124231.
Cui, H., Bai, J., 2019. A new hyperparameters optimization method for convolutional neural networks. Pattern Recogn. Lett. 125, 828–834.
Daniel, E., Anitha, J., Gnanaraj, J., 2017. Optimum laplacian wavelet mask based medical image using hybrid cuckoo search–grey wolf optimization algorithm. Knowl.-Based Syst. 131, 58–69.
Darabi, H., Choubin, B., Rahmati, O., Haghighi, A.T., Pradhan, B., Kløve, B., 2019. Urban flood risk mapping using the GARP and QUEST models: A comparative study of machine learning techniques. J. Hydrol. 569, 142–154.
Deb, K., 2012. Optimization for engineering design: Algorithms and examples. PHI Learning Pvt. Ltd.
Demolli, H., Dokuz, A.S., Ecemis, A., Gokcek, M., 2019. Wind power forecasting based on daily wind speed data using machine learning algorithms. Energy Convers. Manage. 198, 111823.
Di Baldassarre, G., Castellarin, A., Montanari, A., Brath, A., 2009. Probability-weighted hazard maps for comparing different flood risk management strategies: a case study. Nat. Hazards 50 (3), 479–496.
Dong, B., Xia, J., Zhou, M., Deng, S., Ahmadian, R., Falconer, R.A., 2021. Experimental and numerical model studies on flash flood inundation processes over a typical urban street. Adv. Water Resour. 147, 103824.
Du, S., Shi, P., Van Rompaey, A., Wen, J., 2015. Quantifying the impact of impervious surface location on flood peak discharge in urban areas. Nat. Hazards 76 (3), 1457–1471.
Eini, M., Kaboli, H.S., Rashidian, M., Hedayat, H., 2020. Hazard and vulnerability in urban flood risk mapping: Machine learning techniques and considering the role of urban districts. Int. J. Disaster Risk Reduct. 50, 101687.
Erdal, H.I., Karakurt, O., 2013. Advancing monthly streamflow prediction accuracy of CART models using ensemble learning paradigms. J. Hydrol. 477, 119–128.
Falah, F., Rahmati, O., Rostami, M., Ahmadisharaf, E., Daliakopoulos, I.N., Pourghasemi, H.R., 2019. Artificial neural networks for flood susceptibility mapping in data-scarce urban areas. In: Spatial modeling in GIS and R for Earth and Environmental Sciences. Elsevier, pp. 323–336.
Fawcett, T., 2006. An introduction to ROC analysis. Pattern Recogn. Lett. 27 (8), 861–874.
Feng, Q., Liu, J., Gong, J., 2015. Urban flood mapping based on unmanned aerial vehicle remote sensing and random forest classifier-A case of Yuyao, China. Water 7 (4), 1437–1455.
Fernández, D.S., Lutz, M.A., 2010. Urban flood hazard zoning in Tucumán Province, Argentina, using GIS and multicriteria decision analysis. Eng. Geol. 111 (1–4), 90–98.
Fewtrell, T.J., Bates, P.D., Horritt, M., Hunter, N.M., 2008. Evaluating the effect of scale in flood inundation modelling in urban environments. Hydrological Processes: An Int. J. 22 (26), 5107–5118.
Fletcher, M.P., O'Rourke, R., Gaikwad, N., Walters, D.L., Hamilton-Craig, C., 2018. Coronary CT in Australia has high positive predictive value unaffected by site volume: an analysis of 510 positive CTCA scans with invasive angiographic correlation. IJC Heart Vasculature 20, 46–49.
Frattini, P., Crosta, G., Carrara, A., 2010. Techniques for evaluating the performance of landslide susceptibility models. Eng. Geol. 111 (1–4), 62–72.
Glenis, V., Kutija, V., Kilsby, C.G., 2018. A fully hydrodynamic urban flood modelling system representing buildings, green space and interventions. Environ. Modell. Software 109, 272–292.
Guha, D., Roy, P.K., Banerjee, S., 2016. Load frequency control of large scale power system using quasi-oppositional grey wolf optimization algorithm. Eng. Sci. Technol., Int. J. 19 (4), 1693–1713.
Gupta, S., Deep, K., 2020. A memory-based grey wolf optimizer for global optimization tasks. Appl. Soft Comput. 93, 106367.
Hallegatte, S., Ranger, N., Mestre, O., Dumas, P., Corfee-Morlot, J., Herweijer, C., Wood, R.M., 2011. Assessing climate change impacts, sea level rise and storm surge risk in port cities: a case study on Copenhagen. Clim. Change 104 (1), 113–137.
Ho, T.K., 1998. The random subspace method for constructing decision forests. IEEE Trans. Pattern Anal. Mach. Intell. 20 (8), 832–844.
Hosseini, F.S., Choubin, B., Mosavi, A., Nabipour, N., Shamshirband, S., Darabi, H., Haghighi, A.T., 2020. Flash-flood hazard assessment using ensembles and Bayesian-based machine learning models: application of the simulated annealing feature selection method. Sci. Total Environ. 711, 135161. https://doi.org/10.1016/j.scitotenv.2019.135161.
Howard, K., Gerber, R., 2018. Impacts of urban areas and urban growth on groundwater in the Great Lakes Basin of North America. J. Great Lakes Res. 44 (1), 1–13.
Hu, P., Pan, J.S., Chu, S.C., 2020. Improved binary grey wolf optimizer and its application for feature selection. Knowl.-Based Syst. 195, 105746.
Javidrad, F., Nazari, M., 2017. A new hybrid particle swarm and simulated annealing stochastic optimization method. Appl. Soft Comput. 60, 634–654.
Jayabarathi, T., Raghunathan, T., Adarsh, B.R., Suganthan, P.N., 2016. Economic dispatch using hybrid grey wolf optimizer. Energy 111, 630–641.

Jayaprakasam, S., Rahim, S.K.A., Leow, C.Y., 2015. PSOGSA-Explore: A new hybrid metaheuristic approach for beampattern optimization in collaborative beamforming. Appl. Soft Comput. 30, 229–237.
Jia, W., Qin, S., Xue, X., 2019. A generalized neural network for distributed nonsmooth optimization with inequality constraint. Neural Networks 119, 46–56.
Jonkman, S.N., Vrijling, J.K., 2008. Loss of life due to floods. J. Flood Risk Manage. 1 (1), 43–56.
Kim, B., Sanders, B.F., Famiglietti, J.S., Guinot, V., 2015. Urban flood modeling with porous shallow-water equations: A case study of model errors in the presence of anisotropic porosity. J. Hydrol. 523, 680–692.
Komaki, G.M., Kayvanfar, V., 2015. Grey Wolf Optimizer algorithm for the two-stage assembly flow shop scheduling problem with release time. J. Comput. Sci. 8, 109–120.
Landwehr, N., Hall, M., Frank, E. 2003. Logistic model trees. In: European Conference on Machine Learning. Springer, pp. 241–252.
Lee, S., Jun, C.H., 2018. Fast incremental learning of logistic model tree using least angle regression. Expert Syst. Appl. 97, 137–145.
Lee, S., Kim, J.C., Jung, H.S., Lee, M.J., Lee, S., 2017. Spatial prediction of flood susceptibility using random-forest and boosted-tree models in Seoul metropolitan city, Korea. Geomatics, Natural Hazards and Risk 8 (2), 1185–1203.
Liu, D., Li, M., Ji, Y.i., Fu, Q., Li, M., Abrar Faiz, M., Ali, S., Li, T., Cui, S., Imran Khan, M., 2020. Spatial-temporal characteristics analysis of water resource system resilience in irrigation areas based on a support vector machine model optimized by the modified gray wolf algorithm. J. Hydrol. 597, 125758. https://doi.org/10.1016/j.jhydrol.2020.125758.
Liu, J., Xu, S., Zhang, F., Wang, L., 2017. A hybrid genetic-ant colony optimization algorithm for the optimal path selection. Intelligent Automation & Soft Computing 23 (2), 235–242.
Long, W., 2016. Grey wolf optimizer based on nonlinear adjustment control parameter. In: 4th International Conference on Sensors, Mechatronics and Automation (ICSMA), pp. 643–648.
Madsen, A.L., Jensen, F., Salmerón, A., Langseth, H., Nielsen, T.D., 2017. A parallel algorithm for Bayesian network structure learning from large data sets. Knowl.-Based Syst. 117, 46–55.
Mafarja, M.M., Mirjalili, S., 2017. Hybrid whale optimization algorithm with simulated annealing for feature selection. Neurocomputing 260, 302–312.
Majumder, P., Eldho, T.I., 2020. Artificial neural network and grey wolf optimizer based surrogate simulation-optimization model for groundwater remediation. Water Resour. Manage. 34 (2), 763–783.
Marchi, L., Borga, M., Preciso, E., Gaume, E., 2010. Characterisation of selected extreme flash floods in Europe and implications for flood risk management. J. Hydrol. 394 (1–2), 118–133.
Marler, R.T., Arora, J.S., 2004. Survey of multi-objective optimization methods for engineering. Struct. Multidiscip. Optim. 26 (6), 369–395.
Mirjalili, S., Mirjalili, S.M., Lewis, A., 2014. Grey wolf optimizer. Adv. Eng. Softw. 69, 46–61.
Mosa, M.A., Anwar, A.S., Hamouda, A., 2019. A survey of multiple types of text summarization with their satellite contents based on swarm intelligence optimization algorithms. Knowl.-Based Syst. 163, 518–532.
Neumann, B., Vafeidis, A.T., Zimmermann, J., Nicholls, R.J., 2015. Future coastal population growth and exposure to sea-level rise and coastal flooding-a global assessment. PLoS ONE 10 (3), e0118571.
Niu, P., Niu, S., liu, N., Chang, L., 2019. The defect of the Grey Wolf optimization algorithm and its verification method. Knowl.-Based Syst. 171, 37–43.
Ouma, Y.O., Tateishi, R., 2014. Urban flood vulnerability and risk mapping using integrated multi-parametric AHP and GIS: methodological overview and case study assessment. Water 6 (6), 1515–1545.
Panahi, M., Gayen, A., Pourghasemi, H.R., Rezaie, F., Lee, S., 2020. Spatial prediction of landslide susceptibility using hybrid support vector regression (SVR) and the adaptive neuro-fuzzy inference system (ANFIS) with various metaheuristic algorithms. Sci. Total Environ. 741, 139937. https://doi.org/10.1016/j.scitotenv.2020.139937.
Peyravi, M., Peyvandi, A.A., Khodadadi, A., Marzaleh, M.A., 2019. Flood in the South-West of Iran in 2019; Causes, Problems, Actions and Lesson Learned. Bulletin of Emergency & Trauma 7 (2), 199.
Pham, B.T., Bui, D.T., Prakash, I., 2017. Landslide susceptibility assessment using bagging ensemble based alternating decision trees, logistic regression and J48 decision trees methods: a comparative study. Geotech. Geol. Eng. 35 (6), 2597–2611.
Piotrowski, A.P., Napiorkowski, J.J., 2013. A comparison of methods to avoid overfitting in neural networks training in the case of catchment runoff modelling. J. Hydrol. 476, 97–111.
Pirnia, A., Golshan, M., Darabi, H., Adamowski, J., Rozbeh, S., 2019. Using the Mann-Kendall test and double mass curve method to explore stream flow changes in response to climate and human activities. J. Water Clim. Change 10 (4), 725–742.
Pontius Jr, R.G., Schneider, L.C., 2001. Land-cover change model validation by an ROC method for the Ipswich watershed, Massachusetts, USA. Agric. Ecosyst. Environ. 85 (1–3), 239–248.
Pourghasemi, H.R., Kariminejad, N., Amiri, M., Edalat, M., Zarafshar, M., Blaschke, T., Cerda, A., 2020. Assessing and mapping multi-hazard risk susceptibility using a machine learning technique. Sci. Rep. 10 (1), 1–11.
Qasim, T., Bhatti, N., 2019. A hybrid swarm intelligence based approach for abnormal event detection in crowded environments. Pattern Recogn. Lett. 128, 220–225.
Rahmati, O., Darabi, H., Haghighi, A.T., Stefanidis, S., Kornejady, A., Nalivan, O.A., Tien Bui, D., 2019. Urban Flood Hazard Modeling Using Self-Organizing Map Neural Network. Water 11 (11), 2370.
Rahmati, O., Darabi, H., Panahi, M., Kalantari, Z., Naghibi, S.A., Ferreira, C.S.S., Kornejady, A., Karimidastenaei, Z., Mohammadi, F., Stefanidis, S., Bui, D.T., Haghighi, A.T., 2020. Development of novel hybridized models for urban flood susceptibility mapping. Sci. Rep. 10 (1), 1–19.
Schmitt, T.G., Thomas, M., Ettrich, N., 2004. Analysis and modeling of flooding in urban drainage systems. J. Hydrol. 299 (3–4), 300–311.
Schubert, J.E., Sanders, B.F., 2012. Building treatments for urban flood inundation models and implications for predictive skill and modeling efficiency. Adv. Water Resour. 41, 49–64.
Şenel, F.A., Gökçe, F., Yüksel, A.S., Yiğit, T., 2019. A novel hybrid PSO–GWO algorithm for optimization problems. Engineering with Computers 35 (4), 1359–1373.
Sessarego, M., Feng, J.u., Ramos-García, N., Horcas, S.G., 2020. Design optimization of a curved wind turbine blade using neural networks and an aero-elastic vortex method under turbulent inflow. Renewable Energy 146, 1524–1535.
Sharifinia, Z., 2019. Assessing the Social Resilience of Rural Areas against Flooding using FANP and WASPAS Models (Case Study: Chardange District of Sari County). Geography Environ. Hazards 8 (30), 1–26.
Shirwaikar, R.D., Acharya, D., Makkithaya, K., Surulivelrajan, M., Srivastava, S., 2019. Optimizing neural networks for medical data sets: A case study on neonatal apnea prediction. Artif. Intell. Med. 98, 59–76.
Shuster, W.D., Bonta, J., Thurston, H., Warnemuende, E., Smith, D.R., 2005. Impacts of impervious surface on watershed hydrology: A review. Urban Water J. 2 (4), 263–275.
Tan, K., Wang, H., Chen, L., Du, Q., Du, P., Pan, C., 2020. Estimation of the spatial distribution of heavy metal in agricultural soils using airborne hyperspectral imaging and random forest. J. Hazard. Mater. 382, 120987. https://doi.org/10.1016/j.jhazmat.2019.120987.
Tehrany, M.S., Pradhan, B., Mansor, S., Ahmad, N., 2015. Flood susceptibility assessment using GIS-based support vector machine model with different kernel types. Catena 125, 91–101.
Tikhamarine, Y., Souag-Gamane, D., Ahmed, A.N., Kisi, O., El-Shafie, A., 2020. Improving artificial intelligence models accuracy for monthly streamflow forecasting using grey Wolf optimization (GWO) algorithm. J. Hydrol. 582, 124435.
Torres, M.A., Jaimes, M.A., Reinoso, E., Ordaz, M., 2014. Event-based approach for probabilistic flood risk assessment. International Journal of River Basin Management 12 (4), 377–389.
Wen, H., Sang, S., Qiu, C., Du, X., Zhu, X., Shi, Q., 2019. A new optimization method of wind turbine airfoil performance based on Bessel equation and GABP artificial neural network. Energy 187, 116106.
Xing, J., Luo, K., Wang, H., Fan, J., 2019. Estimating biomass major chemical constituents from ultimate analysis using a random forest model. Bioresour. Technol. 288, 121541.
Yagiura, M., Ibaraki, T., 2001. On metaheuristic algorithms for combinatorial optimization problems. Systems Computers Japan 32 (3), 33–55.
Yang, X.S., 2014. Swarm intelligence-based algorithms: a critical analysis. Evol. Intel. 7 (1), 17–28.
Yu, S., Lu, H., 2018. An integrated model of water resources optimization allocation based on projection pursuit model–Grey wolf optimization method in a transboundary river basin. J. Hydrol. 559, 156–165.
Zedadra, O., Guerrieri, A., Jouandeau, N., Spezzano, G., Seridi, H., Fortino, G., 2018. Swarm intelligence-based algorithms within IoT-based systems: A review. J. Parallel Distrib. Comput. 122, 173–187.
Zhang, Y., Jin, Z., Chen, Y., 2020. Hybrid teaching–learning-based optimization and neural network algorithm for engineering design optimization problems. Knowl.-Based Syst. 187, 104836.
Zhao, B., Ren, Y.i., Gao, D., Xu, L., Zhang, Y., 2019. Energy utilization efficiency evaluation model of refining unit Based on Contourlet neural network optimized by improved grey optimization algorithm. Energy 185, 1032–1044.
Zhao, G., Pang, B., Xu, Z., Yue, J., Tu, T., 2018. Mapping flood susceptibility in mountainous areas on a national scale in China. Sci. Total Environ. 615, 1133–1142.
Zhao, Y., Zhang, Y., 2008. Comparison of decision tree methods for finding active objects. Adv. Space Res. 41 (12), 1955–1959.
Zhao, Y., Li, Y., Zhang, L., Wang, Q., 2016. Groundwater level prediction of landslide based on classification and regression tree. Geod. Geodyn. 7 (5), 348–355.